CSIRO PUBLISHING

International Journal of Wildland Fire
http://dx.doi.org/10.1071/WF16106

Hillslope-scale prediction of terrain and forest canopy effects on temperature and near-surface soil moisture deficit

Sean F. Walsh[A,D], *Petter Nyman*[B], *Gary J. Sheridan*[B], *Craig C. Baillie*[B], *Kevin G. Tolhurst*[C] *and Thomas J. Duff*[A]

[A]School of Ecosystem and Forest Sciences, University of Melbourne, Burnley Campus, 500 Yarra Boulevard, Richmond, Vic. 3121, Australia.
[B]School of Ecosystem and Forest Sciences, University of Melbourne, Parkville Campus, Grattan Street, Parkville, Vic. 3010, Australia.
[C]School of Ecosystem and Forest Sciences, University of Melbourne, Creswick Campus, Water Street, Creswick, Vic. 3363, Australia.
[D]Corresponding author. Email: seanfwalsh.research@gmail.com

Abstract. Soil moisture has important effects on fuel availability, but is often assessed using drought indices at coarse spatial resolution, without accounting for the fine-scale spatial effects of terrain and canopy variation on forest floor moisture. In this study, we examined the spatial variability of air temperature, litter temperature and near-surface soil moisture (θ, 0–100 mm) using data from field experiments at 17 sites in south-east Australia, covering a range of topographic aspects and vegetation types, within climates from semiarid to wet montane. Temperatures and θ in mountainous environments were found to vary at much finer spatial scales than typical drought index grid dimensions (several kilometres). Using terrain elevation, local insolation ratio and plant area index, we developed semi-empirical microclimate models for air and litter temperatures, then used modelled temperatures as input into calculations of the Keetch–Byram Drought Index, a widely used index of soil moisture deficit. Drought index results based on predicted litter temperature were found to explain 91% of the spatial variation in near-surface soil moisture at our experimental sites. These results suggest the potential for routine hillslope-scale predictions of forest floor moisture status, which may be useful in the management of fire, particularly prescribed burning, in complex terrain.

Additional keywords: complex terrain, downscaling, drought index, KBDI, microclimate.

Received 9 June 2016, accepted 4 January 2017, published online 16 February 2017

Introduction

Background

Forest fires exhibit complex behaviour, partly because of strong spatial and temporal variation in the key factors affecting fire behaviour, including meteorology (Bradstock *et al.* 2010), topography (Sharples 2009; Schunk *et al.* 2013), barriers to fire propagation (Agee *et al.* 2000), extent of suppression effort (Martell and Sun 2008) and fine-fuel moisture content (Anderson and Rothermel 1965; Van Wagner 1987). These factors can be difficult to predict at high spatial and temporal resolution, creating challenges for modelling at hillslope scales.

The prediction of fine dead fuel moisture content is especially challenging and has been the subject of extensive research (Matthews 2014). Litter fine-fuel moisture and availability vary over short time scales (typically hours) through absorption and desorption of atmospheric moisture (Viney 1991; Slijepcevic *et al.* 2013) and over longer time scales (days to weeks) through the influence of soil moisture and precipitation (McArthur 1967). Soil moisture is also important in determining the moisture content and flammability of live fuels (Pellizzaro *et al.* 2007; Krueger *et al.* 2016).

Consequently, forest fire prediction systems typically rely on information about soil moisture status as a key input into fire behaviour calculations, usually in the form of a moisture deficit (the amount of water that must be added to bring the soil up to field capacity). Soil moisture status can be predicted with dynamical models that account for canopy rainfall interception, soil infiltration and evapotranspiration (e.g. Lee *et al.* 2007; Cáceres *et al.* 2015), although such models are rarely used in operational fire prediction where rapid calculations are required. Instead, it is common practice to estimate soil moisture deficit using a drought index, such as the Nesterov Index (Nesterov 1949; Groisman *et al.* 2007), the Canadian moisture codes (Van Wagner 1987), or the Keetch–Byram Drought Index (KBDI; Keetch and Byram 1968).

Drought indices such as these are typically generated by weather forecasting or fire management agencies over large regions using a grid resolution of several kilometres

Table 1. Keetch–Byram Drought Index (KBDI) assumptions regarding moisture input, loss and retention processes

Process	Assumptions
Moisture input	Soil water recharge occurs through rainfall with an adjustment for interception losses, assumed to occur in the canopy; litter interception is not explicitly considered. A fixed interception threshold of 5 mm is assumed, below which effective rainfall is set to zero. In the case of consecutive days of rain, with insufficient time for the canopy to dry between showers, the 5 mm is only subtracted once, on the first day when cumulative rainfall exceeds 5 mm.
Moisture loss	The daily rate of soil water loss is modelled with an evapotranspiration (ET) function, where transpiration is assumed to be the major component of ET. There is no explicit treatment of evaporation from soil, surface runoff or deep drainage, but saturation excess runoff is implicitly handled by discarding additional water input once the index has reached zero. Post-rainfall ET is assumed to follow an exponential decay curve in the absence of further rain. Spatial variation in ET is modelled using a function of mean annual rainfall, acting as a proxy for vegetation density and thus transpiration rate. Temporal variation in ET is modelled using only daily maximum temperature and the previous daily estimate of moisture deficit; wind speed, vapour pressure deficit and solar radiation are not considered.
Moisture retention	Soil moisture is assumed to be held within an abstract quantity of soil, duff or litter, considered to have a field capacity of 203 mm (8 inches). The index ranges from 0 mm (soil at field capacity) to 203 mm (maximum deficit, indicating wilting point). Actual soil depth and porosity are not considered.

(Riley *et al.* 2013). This provides a useful regional overview, but is unable to represent hillslope-scale variation due to changes in aspect, vegetation density or soil type (Sharples 2009; Nyman *et al.* 2014). Fuel moisture plays a critical role in the outcome of prescribed burning (Burgan 1987; Reid *et al.* 2012), and needs to be quantified at a fine spatial scale for burn simulations to be effective (Ferguson *et al.* 2001). As soil moisture is known to influence fuel moisture and fuel availability, particularly in the lower layers of forest litter (Hatton *et al.* 1988), this indicates the need to reduce the spatial scale of gridded soil moisture products, while retaining sufficient spatial coverage to support regional fire risk management.

In practice, the prediction of soil moisture status at a desired target resolution is not straightforward as the most relevant predictors depend on the spatial scale of interest, from broad climatic gradients at continental scale (~1000 km), to soil and vegetation type variation at intermediate scales (~10–100 km) and terrain and vegetation density at hillslope scales (Western *et al.* 2002). Key processes affecting spatial patterns may also depend on seasonal dynamics, with local-scale factors having a greater influence during dry periods (Grayson *et al.* 1997). Consequently, soil moisture exhibits considerable spatial complexity (Svetlitchnyi *et al.* 2003; Busch *et al.* 2012; Korres *et al.* 2015).

Downscaling soil moisture information to hillslope scale can be achieved through detailed modelling of moisture dynamics (e.g. Running 1991; Kang *et al.* 2004). However, this requires extensive calibration and parameterisation of several submodels over the region of interest. Here an alternative approach is used, starting with a simple drought index and developing modifications to account for spatial variation in the drying rate at hillslope scale. For this purpose, we chose the KBDI, a widely used index of soil moisture deficit (Keetch and Byram 1968).

The KBDI is a simple moisture budget model, intended to represent the effect of drought on forest fires burning in deep duff and upper soil layers containing organic matter (Keetch and Byram 1968). Although model parameters were developed using data from a single region (south-eastern USA; Nelson (1959)), it is common practice for the index to be used in a largely unaltered form across many continents and forest types (Janis *et al.* 2002; Dolling *et al.* 2005; Liu *et al.* 2010; Lucas 2010; Varol and Ertuğrul 2016). The key assumptions behind the KBDI are listed in Table 1.

Operational fire management efforts in the USA and Australia rely on routine calculations of the KBDI, which is used as a general indication of forest dryness. In several Australian states, the KBDI is an input into calculations of dead fuel availability (Finkele *et al.* 2006), which in turn is used to estimate fire danger and rates of spread (McArthur 1967; Noble *et al.* 1980). There is some evidence that the KBDI performs well in predicting live fuel moisture (Dimitrakopoulos and Bemmerzouk 2003) and the water potential of live plant material (Xanthopoulos *et al.* 2006), but poorly in predicting dead litter moisture (de Dios *et al.* 2015).

Given the critical importance of forest litter in fire behaviour (Sullivan *et al.* 2012), and the link between moisture in near-surface soil and litter (Hatton *et al.* 1988), this suggests the need to develop specific indicators of moisture (or moisture deficit) in near-surface soil, defined here as soil to a depth of 100 mm. In addition to its effects on litter, moisture in this soil layer may have a substantial influence over the live fuel moisture in near-surface vegetation, which also plays a key role in forest fire behaviour (Cheney *et al.* 2012).

Nyman *et al.* (2015*b*) proposed indicators based on the KBDI but using air or litter temperatures under the forest canopy, instead of air temperature measured in standard open conditions. This effectively alters the drying rate in the KBDI soil moisture budget, with below-canopy temperatures providing an indication of near-surface water loss processes such as evaporation and transpiration by grasses and other shallow-rooted vegetation. When combined with microclimate models for forest air and litter temperatures, this approach allows predictions of near-surface soil moisture deficit at the hillslope scale, which can be tested against field measurements of soil moisture.

Research objectives

The purpose of this study is to illustrate the first-order spatial effects of complex terrain and canopy density variation on

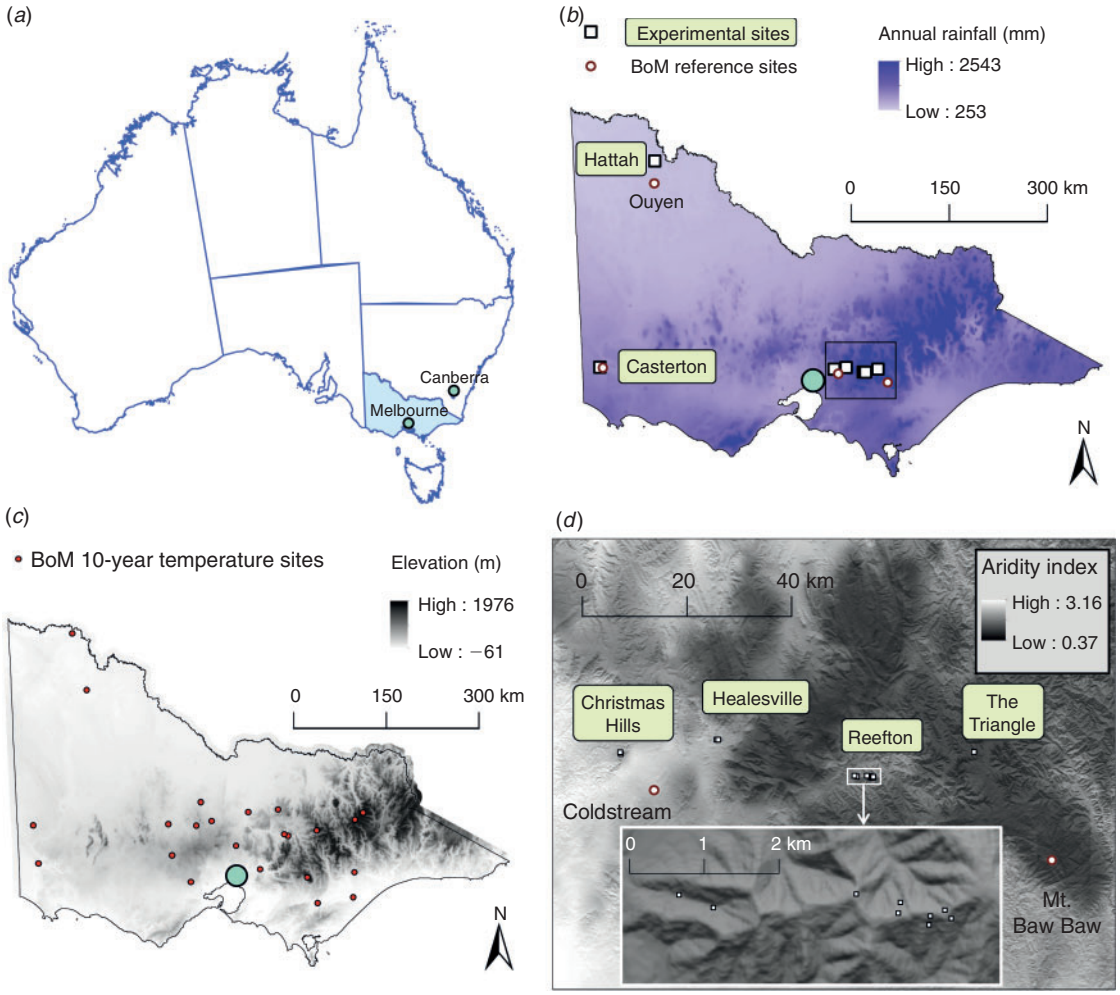

Fig. 1. Study area and site locations in relation to climate and topography. (*a*) Outline of the Australian continent with the state of Victoria shown in the south-east. (*b*) Annual average rainfall and the location of experimental sites and Bureau of Meteorology (BoM) reference sites. A rectangle highlights sites east of Melbourne along an orographic rainfall gradient. (*c*) Elevation map of Victoria showing 23 BoM sites chosen for determination of a local lapse rate (see Eqn 4). (*d*) Close-up view of rainfall gradient sites, with greyscale indicating the Budyko radiative index of dryness (aridity) as described in Nyman *et al.* (2014), and inset providing further detail of experimental sites in the Reefton area.

temperature and near-surface soil moisture deficit, by using simple semi-empirical models supported by field measurements. This work aims to support the development of tools that can be applied by fire managers in complex terrain using widely available data as input. Specifically, this research seeks to:

- use field experiments to investigate the extent of hillslope-scale spatial variation in near-surface soil moisture, air temperature and litter temperature in natural forests within complex terrain;
- develop simple microclimate models for below-canopy air and litter temperature, and parameterise these models using field measurements and readily available weather data;
- investigate whether the use of these modelled temperatures in calculating the KBDI enables effective prediction of the spatial variability in near-surface soil moisture.

Materials and methods

Study area

Experiments were conducted in forests and woodlands of Victoria, in south-east Australia (Fig. 1*a*). Climate in this region varies from alpine to semiarid, with most areas experiencing a mediterranean climate with relatively cool, wet winters (June–August) and hot, dry summers (December–February). Mean annual temperature in Victoria ranges from 4 to 17°C, and precipitation ranges from ~250 to 2500 mm year^{-1} (Fig. 1*b*), with greater rainfall in coastal mountain ranges and high-elevation areas. Locations with rainfall of more than 800 mm year^{-1} support dry to wet temperate eucalypt forests, with lower-rainfall areas supporting more drought-tolerant vegetation types including open woodland, heathy woodland and mallee.

The terrain across the study area is highly variable (Fig. 1*c*), with the Great Dividing Range (reaching from the central west

to the north-east) resulting in strong orographic effects on rainfall (Fig. 1*b*). Terrain elevation along the main ridge of the divide increases from ~500 m (above sea level) in the central west to just under 2000 m in the north-east, and within this mountainous region, changes in rainfall and elevation interact to create substantial variability in vegetation. Where rainfall is >1200 mm year^{-1} and elevation is <1500 m, forests are typically dominated by tall species such as mountain ash (*Eucalyptus regnans* F. Muell.) or alpine ash (*E. delegatensis* R. T. Baker). Areas with lower rainfall (800–1200 mm year^{-1}) contain more open forest supporting a wider range of eucalypt species. The complex terrain in these ranges also produces strong heterogeneity in vegetation, due to differences in insolation caused by variations in slope, aspect and terrain shading (Nyman *et al.* 2014).

Fire is an integral aspect of vegetation ecology in this region (Gill *et al.* 1981), and wildfires are a major risk to communities and assets (Blanchi *et al.* 2006). Fire regimes vary with vegetation type, with fire-tolerant vegetation in the drier areas adapted to frequent burning (Noble and Slatyer 1981). Tall temperate forests, generally in the eastern part of the state, are prone to infrequent stand-replacing fires that burn primarily during extreme fire conditions (Bradstock 2008). In open woodlands and mallee in the western part of the state, the fire regime is more complex and variable, with some areas experiencing very long inter-fire intervals (Clarke *et al.* 2010).

Sites and instrumentation

Field data were taken from three related experiments conducted between December 2013 and August 2015. These experiments involved six locations in south-east Australia (Hattah, Casterton, Christmas Hills, Healesville, Reefton and The Triangle), as shown in Fig. 1. Measurements included below-canopy air temperature, litter temperature and near-surface soil moisture in settings with contrasting vegetation, topographic aspect and hillslope position.

Sites were chosen to support the development of models for downscaling regional weather observations or forecasts to local conditions below the canopy at 20-m resolution, making use of a digital elevation model (DEM) and vegetation attributes. At regional scales, rainfall is the main source of variation, so the six locations were established to cover a wide range of mean annual rainfall values (from 323 mm at Hattah to 1745 mm at The Triangle). The local-scale effects of topographic aspect and hillslope position were examined by locating sites at different aspects and hillslope positions. A total of 17 sites were established (Table 2) in areas supporting a range of Ecological Vegetation Classes (Cheal 2010).

Two locations (Hattah and Casterton) are within very flat terrain in the west of the state, with the remaining locations (Christmas Hills, Healesville, Reefton and The Triangle (Fig. 1*d*)) in mountainous terrain. A single site was placed at each of the flat-terrain locations. At Christmas Hills, Healesville and The Triangle, paired sites were placed on nearby north (equatorial) and south (polar) facing hillslopes. At Reefton, sites were placed at three hillslope positions ('upper', 'midslope' and 'drainage') on both north and south facing slopes (Fig. 1*d*, inset), encompassing contributing areas ranging from 760 to 18 800 m^2. Three sites from a previous study in the Upper Yarra catchment at Reefton (Nyman *et al.* 2015*b*) provided east and west aspects plus an additional south facing site.

At each site, hemispherical photographs were taken either early or late in the day to avoid interference from direct sunlight. The photographic system consisted of a Coolpix 8400 camera fitted with an FC-E9 fisheye lens and UR-E16 adaptor ring (Nikon Corporation), and a SLM6 self-levelling mount (Delta-T Devices). Plant Area Index (*PAI*) was calculated from each image using the *HemiView* software system (Rich *et al.* 1999). Mean annual rainfall data were obtained from a previous study that interpolated long-term rainfall records in Victoria (Nyman *et al.* 2014).

Screen-level air temperature (T_{SLA}) at 1.5 m above the forest floor was measured using a Campbell CS215 probe. Temperature within the litter layer (T_{LIT}) was measured as the average of readings in four litter packs at ground level, constructed from PVC pipe 40 mm deep and 240 mm in diameter (Nyman *et al.* 2015*a*). Temperature readings were taken as 30-minute averages, which were processed to form daily maxima. For each experimental site, a reference site was determined as the nearest Bureau of Meteorology (BoM) station with temperature data (Table 3), and for each reference site, daily maximum temperature data were obtained for the period 1 July 2013 to 31 August 2015.

Volumetric near-surface soil moisture fraction (θ) was measured using two moisture probes (Delta-T Devices) at each site, averaged to provide a single time series. At most sites, ML3-type probes were used, buried to a depth of ~50 mm. At the four Reefton Aspect sites (Table 2), ML2x-type probes were used at a depth of ~60 mm, and at Hattah and Casterton, SM150-type probes were used at a depth of ~75 mm. Probes were calibrated using manual soil moisture measurements as described in Nyman *et al.* (2015*b*), except at Hattah and Casterton, where the factory calibration for mineral soil was used. Given the uncertainty in precisely delineating the upper horizons in typical forest soils (Boone *et al.* 1999), all calibrated probe results were considered to represent the average moisture in the top 100 mm of soil. At each site, raw 30-minute averages were converted to daily averages.

Analysis and modelling approach

Modifications to the KBDI

A metric version of the KBDI was used, incorporating the corrections noted by Alexander (1990):

$$ET(t) = \frac{(203 - \mathrm{KBDI}(t-1))(0.9681e^{(0.08748\,T_{MAX}(t)+1.555)} - 8.292)}{1000(1 + 10.88e^{-0.001736\bar{P}})} \quad (1)$$

$$\mathrm{KBDI}(t) = \mathrm{KBDI}(t-1) - P_{eff}(t) + ET(t) \quad [\min = 0, \max = 203\,\mathrm{mm}] \quad (2)$$

The moisture-loss term $ET(t)$ is the daily evapotranspiration on day t, which is modelled as a function of long-term mean annual rainfall ($\bar{P}$), daily maximum temperature ($T_{MAX}(t)$), and

Table 2. Experimental site attributes

Shortwave insolation ratio, slope, elevation, aspect, contributing area and aridity are based on a 20-m digital elevation model (DEM), with further details provided in Nyman *et al.* (2014). Mean annual rainfall was obtained from long-term observations interpolated by Nyman *et al.* (2014). Ecological Vegetation Class (EVC) was extracted from data described in Cheal (2010). The Hattah and Casterton sites are from a study of automated fuelsticks (Bovill *et al.* 2015), and the Reefton Aspect series of sites are from Nyman *et al.* (2015*b*); all other sites were commissioned for the current study. Note that sites RAS_N and R_NU are at identical locations. [n/a, not applicable]

Site name	Site code	Data record	Latitude (φ) (degrees)	Shortwave insolation ratio ($\bar{S}$)	Slope (degrees)	Elev. (Z) (m)	Aspect (0–360)	Contrib. area (m^2)	Aridity	Mean annual rainfall ($\bar{P}$) (mm)	Ecological Vegetation Class	Plant Area Index (PAI)
Hattah	HA	Dec 14–Jul 15	−34.7588	1.01	1.3	54	n/a	n/a	7.32	323	Mallee	0.35
Casterton	CA	Dec 14–Jul 15	−37.5751	1.00	0.6	121	n/a	n/a	3.00	694	Heathy woodland	0.74
Healesville North	H_N	Nov 14–Aug 15	−37.6360	1.16	14.2	185	0	980	2.25	1012	Herb-rich foothill forest	2.39
Healesville South	H_S	Nov 14–Aug 15	−37.6357	0.81	18.9	185	206	1060	1.69	1017	Damp forest	2.68
Christmas Hills North	C_N	Nov 14–Aug 15	−37.6612	1.16	14.8	285	31	1040	2.17	1039	Grassy dry forest	1.73
Christmas Hills South	C_S	Nov 14–Aug 15	−37.6584	0.80	16.7	260	164	1540	1.61	1041	Valley grassy forest	2.08
Reefton North Upper	R_NU	Nov 14–Aug 15	−37.6983	1.29	18.1	620	8	760	1.92	1272	Heathy dry forest	1.97
Reefton North Midslope	R_NM	Nov 14–Aug 15	−37.6970	1.28	30.8	535	22	3640	1.88	1271	Shrubby foothill forest	2.36
Reefton North Drainage	R_ND	Nov 14–Aug 15	−37.6978	1.19	23.6	340	345	14400	1.76	1289	Damp forest	3.10
Reefton South Upper	R_SU	Nov 14–Aug 15	−37.6986	0.74	26.4	608	193	840	1.24	1274	Wet forest	4.22
Reefton South Midslope	R_SM	Nov 14–Aug 15	−37.6997	0.79	21.6	549	161	3260	1.29	1274	Wet forest	5.31
Reefton South Drainage	R_SD	Nov 14–Aug 15	−37.6963	0.92	9.5	308	222	18 800	1.45	1297	Damp forest	3.41
Reefton Aspect North	RAS_N	Dec 13–Nov 14										
Reefton Aspect South	RAS_S	Dec 13–Nov 14	−37.6989	0.83	24.0	610	155	1440	1.35	1276	Wet forest	3.99
Reefton Aspect East	RAS_E	Dec 13–Nov 14	−37.6961	1.11	24.2	611	70	920	1.70	1270	Shrubby foothill forest	2.12
Reefton Aspect West	RAS_W	Dec 13–Nov 14	−37.6979	1.16	16.8	620	293	960	1.77	1273	Damp forest	2.21
The Triangle North	T_N	Nov 14–Aug 15	−37.6530	1.18	10.7	1065	347	680	1.31	1745	Montane damp forest	3.35
The Triangle South	T_S	Nov 14–Aug 15	−37.6536	1.00	7.6	1064	228	660	1.15	1745	Montane wet forest	3.78

Table 3. Bureau of Meteorology (BoM) reference sites

Reference sites for each experimental location are selected as the nearest BoM site with temperature data. Shortwave insolation ratio, slope and elevation are based on a 20-m digital elevation model (DEM). Distances and elevation differences are shown as a range over all experimental sites at a given location

Experimental location	Reference site	Reference site details				Distance from reference site to experimental sites	Elevation difference between reference and experimental sites ($Z - Z_{REF}$)
		Latitude (φ_{REF}) (degrees)	Shortwave insolation ratio ($\bar{S}_{REF}$)	Slope (degrees)	Elevation (Z_{REF}) (m)	(km)	(m)
Hattah	Ouyen(BoM)	−35.0682	1.01	2.4	64	34.4	−9
Casterton	Casterton(BoM)	−37.5830	1.00	0.8	134	4.7	−13
Healesville	Coldstream(BoM)	−37.7239	1.00	0.7	83	(range 15.4 : 15.7)	(range 102 : 102)
Christmas Hills	Coldstream(BoM)	−37.7239	1.00	0.7	83	(range 9.4 : 9.8)	(range 177 : 202)
Reefton	Coldstream(BoM)	−37.7239	1.00	0.7	83	(range 38.5 : 42.2)	(range 225 : 537)
The Triangle	Mt Baw Baw(BoM)	−37.8383	1.26	16.6	1560	(range 25.5 : 25.5)	(range −497 : −495)

the previous daily estimate of soil moisture deficit (KBDI($t-1$)). Spatial variations in long-term mean ET are accounted for by using $\bar{P}$ as an indicator of the mean transpiration rate (Keetch and Byram 1968). As the numerator of Eqn 1 becomes negative when temperature falls below 6.8°C, a constraint was applied to ensure $ET(t) \geq 0$.

The moisture-gain term $P_{eff}(t)$ is the daily effective precipitation:

$$P_{eff}(t) = P(t) - I(t) \quad (3)$$

where $P(t)$ is daily precipitation and $I(t)$ represents interception losses determined by a threshold algorithm (described in Table 1).

For each experimental site, four alternative calculations of the KBDI were prepared, depending on the information used for $T_{MAX}(t)$ in Eqn 1:

- K_{REF}, using air temperature (T_{REF}) measured at the nearest reference site (Table 3);
- K_{LOC}, using open-air temperature (T_{LOC}) estimated by adjusting T_{REF} for location (elevation and latitude);
- K_{SLA}, a variant of the KBDI using screen-level air temperature (T_{SLA}); and
- K_{LIT}, a variant of the KBDI using litter layer temperature (T_{LIT}).

The maximum KBDI value (203 mm) is somewhat arbitrary (Keetch and Byram 1968), so the four drought index results were converted to fractional soil moisture deficit values (K = KBDI/203), which were used as approximate estimates of the fractional deficit in near-surface soil. The four K values were then compared with measured volumetric near-surface soil moisture (θ). The K_{REF} metric is essentially the original KBDI in normalised form, and as such is not expected to perform well in predicting near-surface θ, but is included here as a benchmark model.

The KBDI requires an unbroken time series of temperature data. To overcome gaps in measurement data (due to storm damage, etc.) and to enable KBDI calculations over a longer time period than that covered by field measurements, models were designed for T_{LOC}, T_{SLA} and T_{LIT} that make use of BoM reference sites, which provide very reliable time series data for temperature.

Air and litter temperature

Observed temperatures on north and south facing aspects were compared, using data from four locations (Christmas Hills, Healesville, Reefton and The Triangle). At Reefton, results from the three hillslope positions (upper, midslope and drainage) were averaged to provide single datasets for north and south facing aspects. A separate comparison was made to examine the effect of varying hillslope position on temperature.

Building on microclimate studies by Running *et al.* (1987), Moore *et al.* (1993), Wilson and Gallant (2000) and Nyman *et al.* (2015*b*), we then developed a simple empirical model suitable for predicting daily maximum air and litter temperature under forest canopies. The model requires a daily maximum temperature measurement or forecast at a reference location (T_{REF}), and applies adjustments to account for:

- differences in elevation and latitude between the reference and target locations (Lee 1978; Rolland 2003);
- the effects of slope, aspect and terrain shading on the amount of shortwave radiation received at the target location, compared with the reference location (Moore *et al.* 1993; Nyman *et al.* 2015*b*); and
- shading caused by the forest canopy, assuming Beer–Lambert extinction of shortwave radiation (Jarvis and Leverenz 1983).

The effects of elevation and latitude were quantified using a 10-year mean of the daily maximum open air temperature ($\bar{T}_{MAX}$), which can be expected to show systematic variation across the landscape. This was modelled as a function of elevation and latitude using an equation from Lee (1978), modified to include a cosine transformation for the latitude term:

$$\bar{T}_{MAX}(Z, \varphi) = A - m_h\, Z + m_\varphi \cos(\varphi) \quad (4)$$

Here Z is elevation above sea level, φ is latitude, and A, m_h and m_φ are parameters to be determined, with the fitted value of m_h providing an environmental lapse rate. Parameters were fitted using Bureau of Meteorology measurements for the period 2005–2014, using weather stations within the study area that

encompass a wide range of altitudes and latitudes. We considered only sites with at least 85% data capture, and excluded sites in the major urban area of Melbourne to avoid the heat-island effect (Torok *et al.* 2001). Twenty-three weather stations in Victoria were identified, with elevations from 4 to 1847 m (Fig. 1*c*).

Eqn 4 was then used to determine the difference in $\bar{T}_{MAX}$ between each experimental site and its matching reference weather station (Table 3):

$$\Delta\bar{T} = m_h(Z_{REF} - Z) + m_\varphi(\cos(\varphi) - \cos(\varphi_{REF})) \quad (5)$$

The effects of slope, aspect and terrain shading on shortwave radiation were calculated in a previous study of Victoria at 20-m resolution using satellite-derived hourly surface irradiance, terrain details and estimates of surface albedo, cloud cover and proportion of diffuse radiation (Nyman *et al.* 2014). Results included a topographic downscaling factor, referred to here as the 'shortwave insolation ratio' (S), which is the total shortwave radiation (direct plus diffuse) received at a specific location divided by the amount expected if the terrain was level at that location (Wilson and Gallant 2000).

Following (Nyman *et al.* 2015*b*), an annual average shortwave insolation ratio ($\bar{S}$) was used to represent the spatial variation in solar energy input. To allow for reference sites that are not on flat terrain, $\bar{S}$ was divided by the annual average insolation ratio at the reference location, giving a simple factor ($\bar{S}/\bar{S}_{REF}$) that was used to relate experimental and reference site temperatures.

The effect of canopy density variation was modelled by applying a further adjustment, in the form of a Beer–Lambert extinction term (Jarvis and Leverenz 1983). Attenuation was assumed to be a function of *PAI*, incorporating the shading effects of stems in addition to leaves.

Combining the effects of location, insolation ratio and canopy shading, we constructed a model as follows:

$$T_{LOC}(t) = T_{REF}(t) + \Delta\bar{T} \quad (6a)$$

$$T(t) = f\,T_{LOC}(t)\left(\frac{\bar{s}}{\bar{s}_{REF}}e^{-k.PAI}\right)^h \quad (6b)$$

where f, k and h are parameters to be fitted, and $T_{LOC}(t)$ refers to air temperature predicted using location effects only (Eqn 5). It was assumed that Eqn 6 could be applied to both screen-level air temperature (T_{SLA}) and litter temperature (T_{LIT}), using separate parameterisations.

Fitting, assessment and comparison of models

Raw temperature data were processed to form daily statistics, using a data capture threshold of 75% to ensure adequate representation of the maximum temperature on each day. The length of the data record varied somewhat among sites (Table 2), so to ensure equal treatment of sites in the model fitting process, a random sample of records was taken from the results for each site. Sample size was determined from the site with the fewest records ($n = 192$ days for air temperature, and $n = 219$ days for litter temperature).

We identified two comparable published models for screen-level air temperature that use T_{REF}, $\bar{S}$ and *PAI* as inputs (Moore *et al.* 1993; Wilson and Gallant 2000), and one model for litter temperature (Nyman *et al.* 2015*b*) that uses T_{REF} and $\bar{S}$ but not *PAI*. Parameters were fitted for all models using non-linear least-squares (*nls*) in *R* (R Development Core Team 2014), and model parsimony was checked using the Akaike Information Criteria (Akaike 1973).

Model performance in predicting an unknown site was assessed using a leave-one-site-out cross-validation. To compare the ability of each model to represent topographic variation, bias and root-mean-square error (RMSE) values were calculated for site groupings based on similar topographic aspect. A sensitivity study was also undertaken to examine the response of each model to systematic changes in $\bar{S}$.

KBDI calculation

At each experimental site, the four normalised metrics (K_{REF}, K_{LOC}, K_{SLA} and K_{LIT}) were calculated daily from 1 July 2013 to 30 June 2015, using measured T_{REF} and model estimates for T_{LOC}, T_{SLA} and T_{LIT} (Eqn 6). At two of the reference sites, Casterton (BoM) and Ouyen(BoM), there were minor gaps in the temperature time series, which were filled using data from the closest BoM stations – Dartmoor (near Casterton) and Walpeup (near Ouyen).

Daily rainfall is measured at BoM reference sites, but these are often at a considerable distance from our experimental locations (Table 3). As rainfall in complex terrain exhibits much greater spatial variability than temperature (Daly *et al.* 2008), time-series data were extracted from the nearest grid centroid in a spatial dataset of interpolated rain gauge measurements (Jones *et al.* 2009), freely available via the Australian Water Resources Audit – Landscape system at 5-km resolution (van Dijk and Renzullo 2011).

All KBDI values were initialised to zero on 1 July 2013 (winter) to ensure initially wet conditions (Fujioka 1991). As the rainfall dataset was derived from measurements to 0900 hours, KBDI calculations were based on a daily update at 0900 hours, requiring the use of the previous day's maximum temperature (Finkele *et al.* 2006). To examine the performance of the four normalised KBDI metrics in predicting spatial variability in θ, a comparison was made between temporally averaged KBDI results and θ measurements at sites where data were available for a comparable time period.

Results

Summary of observations

Near-surface soil moisture

Daily average near-surface θ measurements for all experimental sites are shown in Fig. 2, demonstrating complex temporal dynamics in response to rainfall events, as well as spatial variability, the latter being the focus of this study.

As expected, where paired north and south sites were established, south (polar) facing sites were found to have higher θ than north (equatorial) facing sites (Fig. 2*a–f*). For the Reefton Aspect Study (N, S, E and W aspects), the south facing site showed higher θ, with minimal differences between the other aspects (Fig. 2*g*). At the driest site (Hattah), measured θ was close to zero for extended time periods (Fig. 2*h*). Seasonal

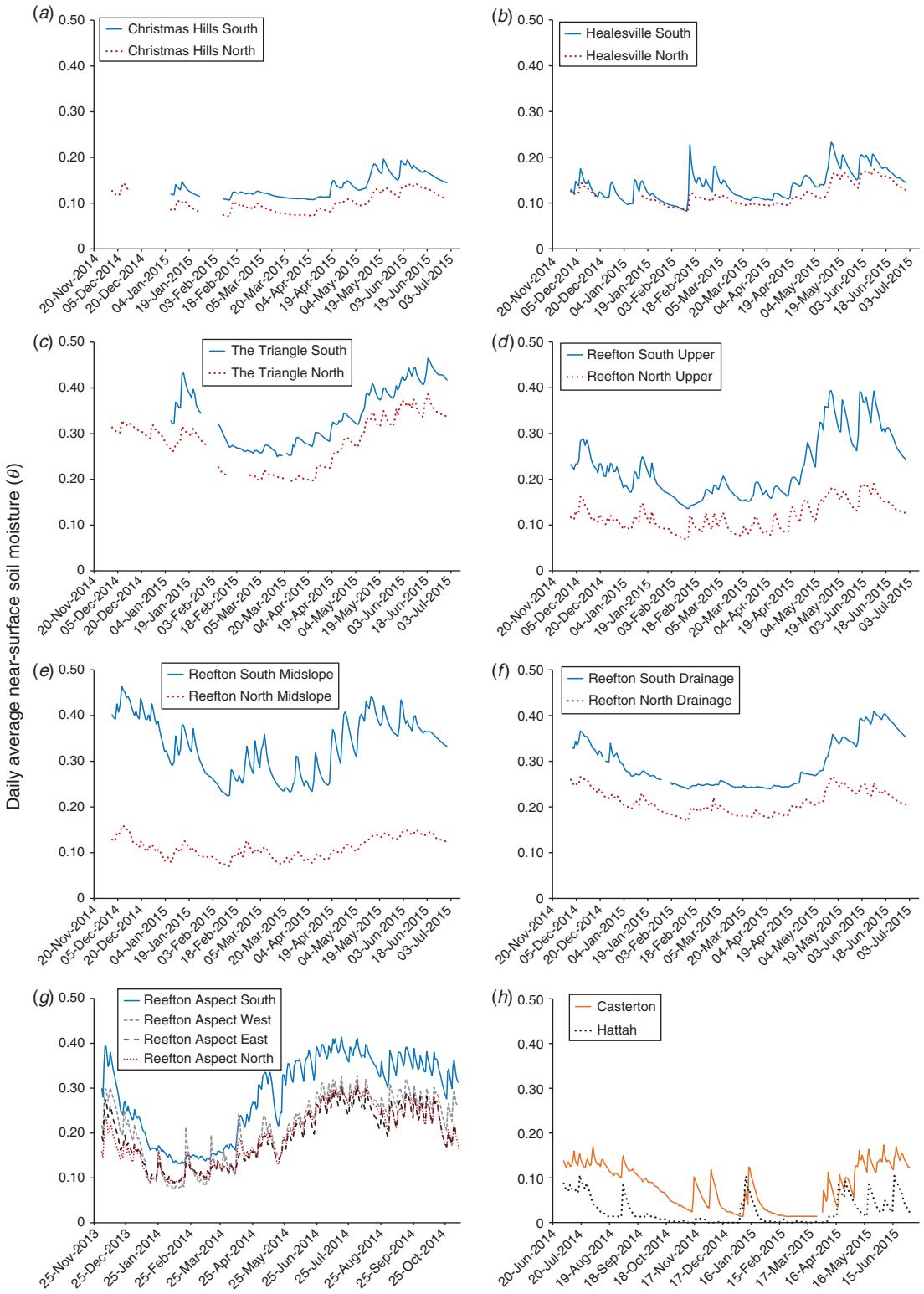

Fig. 2. Daily average near-surface soil moisture measurements. (*a–f*) Comparisons of north and south facing sites at Christmas Hills, Healesville, The Triangle and Reefton from 1 December 2014 to 30 June 2015. (*g*) Comparison of N, S, E and W facing sites at Reefton from 2 December 2013 to 2 November 2014. (*h*) Hattah and Casterton (dry, flat terrain sites) from 1 July 2014 to 2 July 2015.

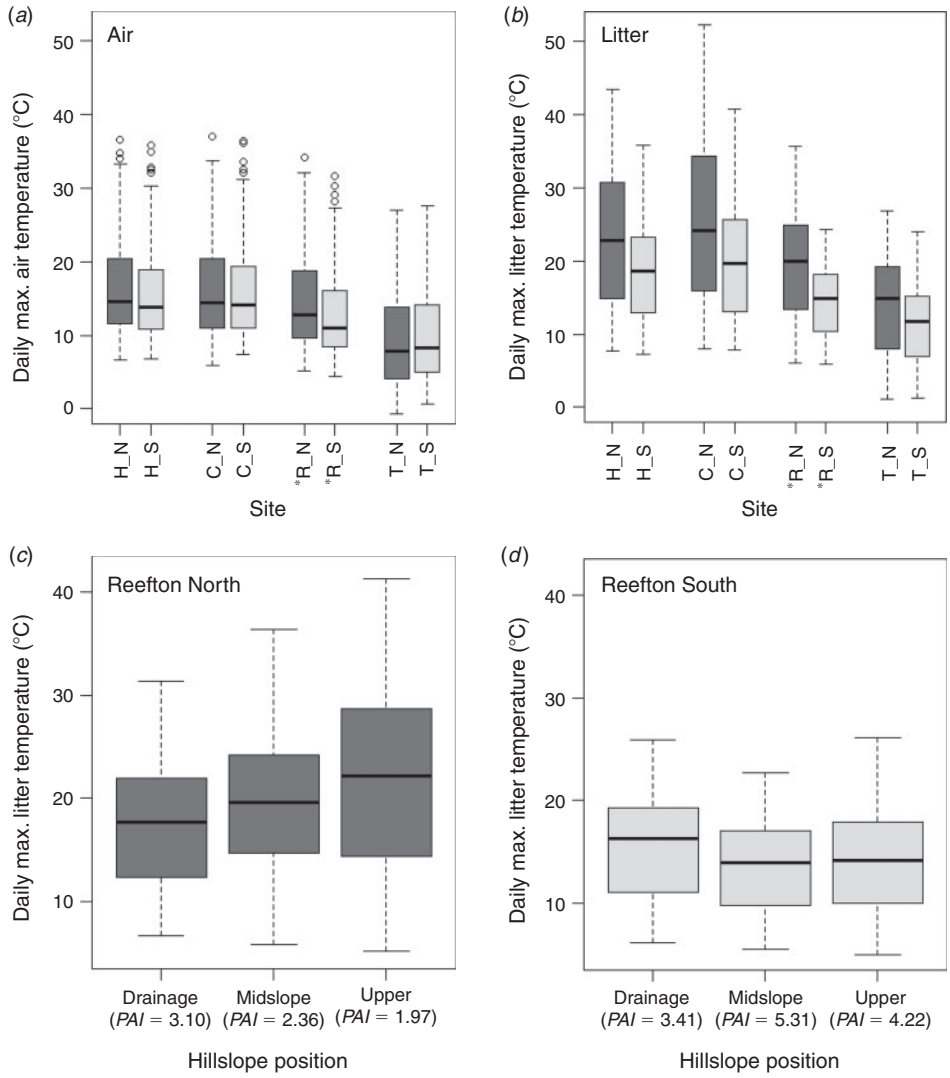

Fig. 3. Daily maximum temperature measurements for the period November 2014 to August 2015. (*a–b*) Comparison of paired north (equatorial) and south (polar) facing sites for (*a*) air; and (*b*) litter temperature; * indicates that Reefton data were averaged over three hillslope positions. (*c–d*) Comparison of litter temperature at different hillslope positions in Reefton for (*c*) north facing; and (*d*) south facing sites.

patterns were as expected, with minimum θ during late summer or early autumn at all sites.

The largest north–south difference in soil moisture was observed at the Reefton midslope sites (Fig. 2*e*), which have substantially different *PAI* values (2.36 vs 5.31) compared with other site pairs. The smallest north–south difference was observed at Healesville, where the *PAI* difference was lowest (2.39 vs 2.68).

At 14 sites (all except the Reefton Aspect series), soil moisture measurements were available for a comparable period (1 December 2014–30 June 2015), with temporal averages varying from 0.02 (Hattah) to 0.34 (The Triangle South). Six of these sites were at Reefton, all within 3.7 km of each other, where average θ varied from 0.11 to 0.33 (71% of the total observed variation), suggesting strong hillslope-scale variability. Across the same six sites, an association was found between $\bar{S}$ and average soil moisture ($r^2 = 0.68$, $n = 6$), with higher values of $\bar{S}$ (more northerly aspects) associated with lower θ.

These results indicate that topographic aspect and canopy density are both important in determining hillslope-scale variation in near-surface θ, and that this local-scale variation is of a similar magnitude to the effects of a substantial climatic gradient.

Temperature

Daily maximum litter temperatures were found to be generally higher than maximum air temperatures (Fig. 3*a–b*), consistent with previous studies of forest microclimate (Geiger *et al.* 1995). At the four locations with paired north and south facing sites (Healesville, Christmas Hills, Reefton and The Triangle), there were distinct north–south differences in litter temperature

Table 4. Screen-level air temperature models: fitted parameters, model bias and Akaike Information Criteria (AIC)
Models by Moore *et al.* (1993) and Wilson and Gallant (2000) have been adapted to use *PAI* instead of *LAI*, and for PAI_{MAX} we have used 5.31, the largest of our measured values (see Table 2)

Model	Origin	Fitted parameters	Bias (°C)	AIC ($\times 10^3$)
$T_{REF}(t)$		n/a	2.3	n/a
$T_{LOC}(t) \equiv T_{REF}(t) + \Delta\bar{T}$	Lee (1978)	n/a	0.6	n/a
$T_{REF}(t) - m_h\Delta z + C\left(\bar{S} - {}^1/_{\bar{S}}\right)\left(1 - {}^{PAI}/_{PAI_{MAX}}\right)$	Wilson and Gallant (2000)	$C = 2.27$	0.7	14.1
$T_{REF}(t) - m_h\Delta z + C\bar{S}\left(1 - {}^{PAI}/_{PAI_{MAX}}\right)$ *for* $\bar{S} > 1$ $T_{REF}(t) - m_h\Delta z - \left({}^{C}/_{\bar{S}}\right)\left(1 + {}^{PAI}/_{PAI_{MAX}}\right)$ *for* $\bar{S} < 1$	Moore *et al.* (1993)	$C = 0.614$	0.3	13.6
$f\,T_{LOC}(t)\left(\left({}^{\bar{S}}/_{\bar{S}_{REF}}\right)e^{-k.PAI}\right)^h$	Proposed model	$f = 1.01$; $h = 0.165$; $k = 0.102$	0.1	13.4

Table 5. Litter temperature models: fitted parameters, model bias and Akaike Information Criteria (AIC)

Model	Origin	Fitted parameters	Bias (°C)	AIC ($\times 10^3$)
$T_{REF}(t)$		n/a	1.2	n/a
$T_{LOC}(t) \equiv T_{REF}(t) + \Delta\bar{T}$	Lee (1978)	n/a	−0.5	n/a
$f\,T_{LOC}(t)\bar{S}^h$	Nyman *et al.* (2015*b*)	$f = 1.02$; $h = 0.621$	0.2	23.3
$f\,T_{LOC}(t)\left(\left({}^{\bar{S}}/_{\bar{S}_{REF}}\right)e^{-k.PAI}\right)^h$	Proposed model	$f = 1.42$; $h = 0.333$; $k = 0.402$	0.0	20.8

(Fig. 3*b*) and more subtle differences in screen-level air temperature (Fig. 3*a*). The highest recorded litter temperature was 52.3°C on 6 February 2015 at Christmas Hills North; on the same day at Christmas Hills South (0.34 km away), litter temperature reached only 32.6°C. At Reefton, litter temperature did not show a clear relationship with hillslope position, but was found to systematically decrease with increasing *PAI* (Fig. 3*c–d*), suggesting that *PAI* may be a more efficient parameter for model development than hillslope position, which has been shown to exert a complex influence on canopy density (Hwang *et al.* 2009; Nyman *et al.* 2015*a*).

Temperature prediction

The 10-year mean of daily maximum temperature across the study area was found to be well predicted via Eqn 4, with adjusted $r^2 = 0.99$. Fitted parameters were $A = -70.7$ (°C), $m_\varphi = 117$ (°C) and $m_h = 7.53$ (°C km^{-1}), with significant effects observed for both elevation and latitude. Results were used in Eqn 5 to determine the mean adjustment for location ($\Delta\bar{T}$) between each experimental site and its matching reference site.

The proposed model and comparable alternatives were parameterised using data from all 17 experimental sites. Fitted parameters, model bias and Akaike Information Criteria (AIC) values are listed in Tables 4 and 5, along with two very simple estimates (T_{REF} and T_{LOC}) that take no account of topographic aspect or canopy density.

Model performance at sites grouped by topographic aspect is summarised in Fig. 4 (bias) and Fig. 5 (RMSE). Compared with the alternatives presented, the proposed model (Eqn 6) was found to have lower overall bias and generally lower bias on specific topographic aspects, for both air and litter temperature. For air temperature, the proposed model performed as well as comparable models in terms of RMSE, and for litter temperature, the proposed model showed lower RMSE than alternative models.

A leave-one-site-out cross-validation found that the proposed screen-level air temperature model was able to explain 90–99% of the variation in T_{SLA} at an unseen site, with an overall r^2 of 0.95. A similar analysis found that the proposed litter temperature model explained 82–92% of the variation in T_{LIT} at an unseen site, with an overall r^2 of 0.87. Detailed cross-validation results are provided in the online supplementary material (Tables S1 and S2).

To further illustrate the response of the model to topographic aspect, model sensitivity to systematic variation in $\bar{S}$ was examined (Fig. 6). Noting that *PAI* may be correlated with radiation input at hillslope scale (Kutiel and Lavee 1999; Sharma *et al.* 2011), a relationship was determined between shortwave insolation ratio and canopy density using nine sites from Reefton ($PAI = 8.02 - 4.68\bar{S}$, $r^2 = 0.77$, $n = 9$), which allowed *PAI* to vary in a realistic manner as $\bar{S}$ was varied. Elevation was kept constant, $\bar{S}_{REF}$ was set to 1.0 and a fixed value of 20°C was used for the model input temperature $T_{LOC}(t)$.

For air temperature, a substantial discontinuity was found at $\bar{S} = 1$ (level ground) in the pair of equations used by Moore *et al.* (1993), equal to twice the fitted constant C, which would predict

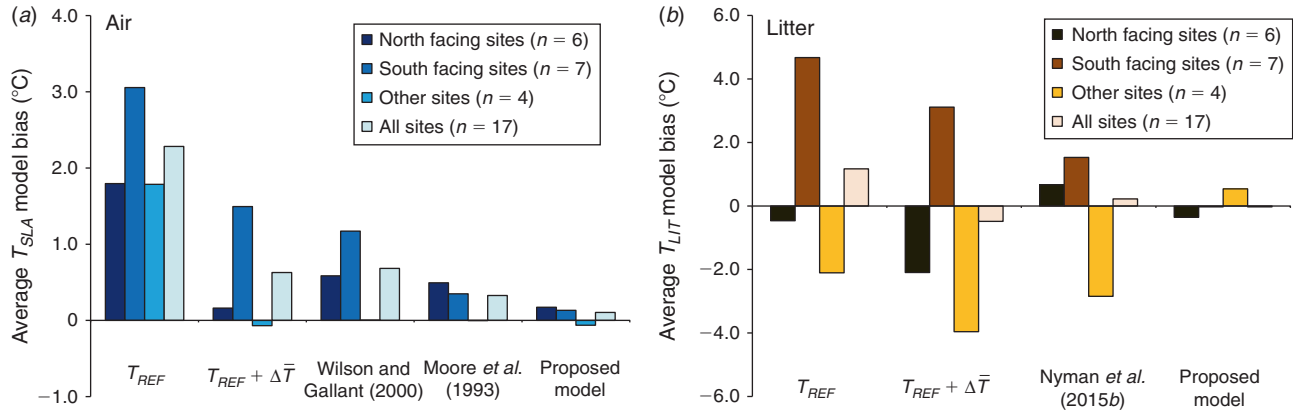

Fig. 4. Model bias for (*a*) screen-level air temperature; and (*b*) litter temperature, calculated over four site groups: north facing sites, south facing sites, other sites (flat, east and west facing) and all sites.

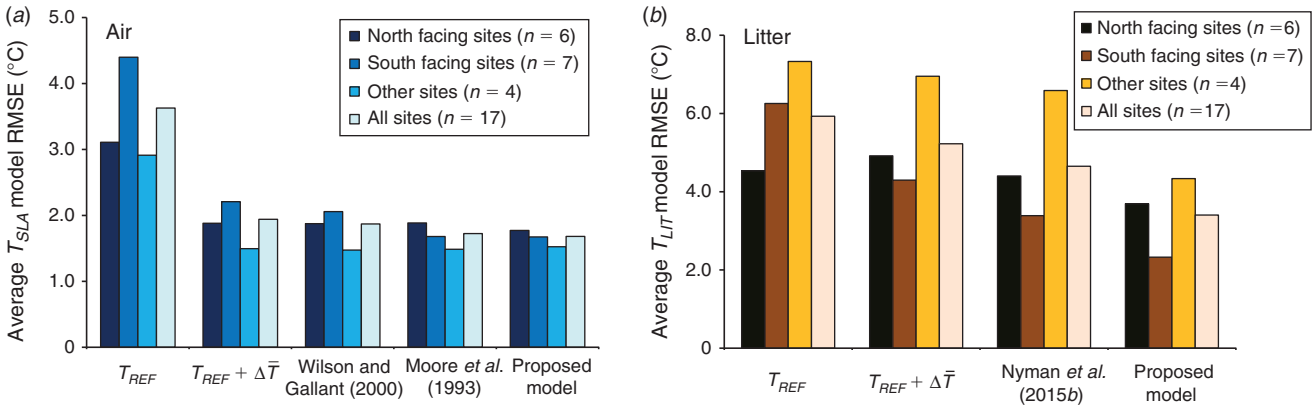

Fig. 5. Model root-mean-square error (RMSE) for (*a*) screen-level air temperature; and (*b*) litter temperature, with sites grouped as for Fig. 4.

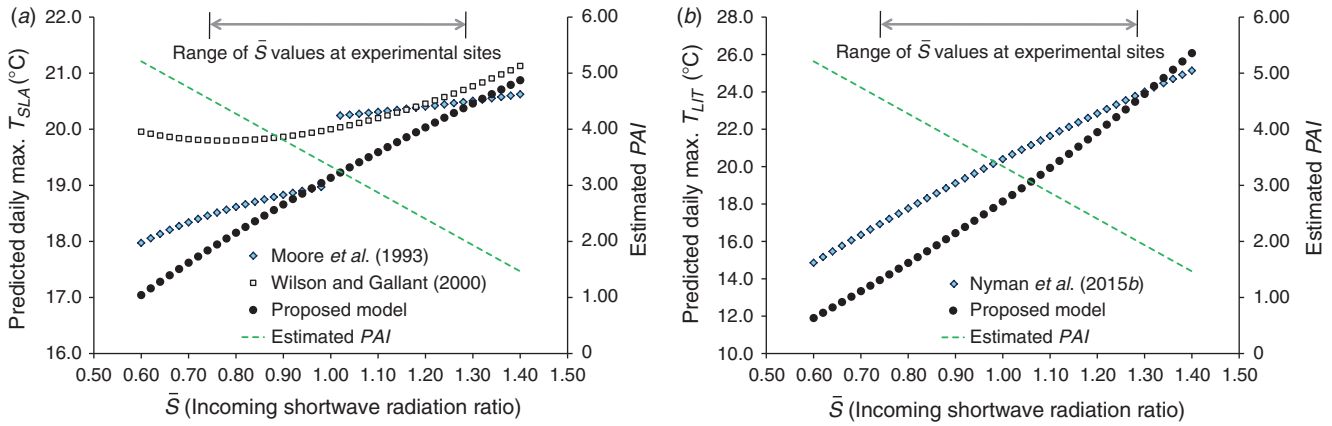

Fig. 6. Model sensitivity to changes in shortwave insolation ratio ($\bar{S}$) for (*a*) screen-level air temperature; and (*b*) litter temperature, with an input temperature (T_{LOC}) of 20°C, and Plant Area Index (*PAI*) allowed to vary with $\bar{S}$ based on a linear regression derived from measurements at nine Reefton sites. For the purposes of this analysis, we considered $\bar{S}$ values from 0.60 to 1.40, a somewhat larger range than was covered by our experimental sites (Table 2). Values of all model parameters (C, f, h, k and PAI_{MAX}) can be found in Tables 4 and 5.

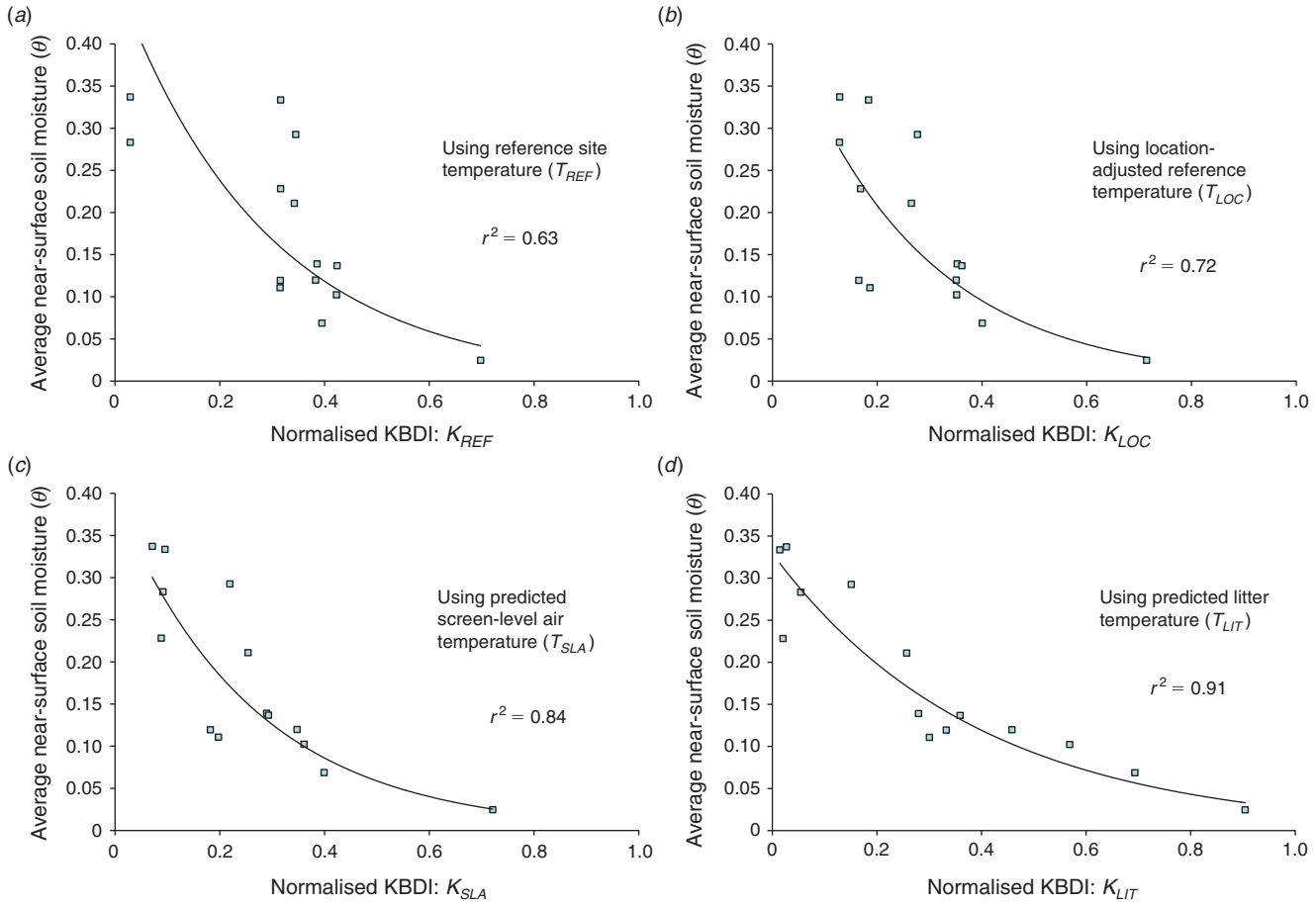

Fig. 7. Field-measured near-surface volumetric soil moisture fraction plotted against normalised Keetch–Byram Drought Index (KBDI) with various temperature treatments. Data represent averages over the period 1 December 2014 to 30 June 2015: (*a*) using nearest Bureau of Meteorology reference temperature with no adjustments; (*b*) using open-air temperature estimated by adjusting reference site temperature for location (elevation and latitude); (*c*) using predicted screen-level air temperature; and (*d*) using predicted litter layer temperature. Fitted curves are of the form $y = ae^{-bx}$ (Nyman *et al.* 2015*b*).

unrealistic step changes in gently undulating terrain. The equation by Wilson and Gallant (2000) removes this discontinuity, but predicts that the canopy has no effect when terrain is level, as $\bar{S} - 1/\bar{S} = 0$. Also, in this test scenario where *PAI* is allowed to increase as $\bar{S}$ decreases, the Wilson and Gallant (2000) model predicts increasing air temperature when $\bar{S}$ is below ~0.75. The proposed model provided a continuously increasing function of $\bar{S}$, consistent with the expected response to solar energy input.

For litter temperature, the proposed model generated lower temperature predictions than Nyman *et al.* (2015*b*), except at high values of $\bar{S}$. On level ground, the fitted model of Nyman *et al.* (2015*b*) predicts that daily maximum litter temperature is always very similar to open-air temperature ($T = 1.02T_{LOC}$). In contrast, the proposed model finds that litter is either warmer or cooler than open-air temperature, depending on canopy density (from Eqn 6, with $\bar{S} = \bar{S}_{REF} = 1$, predicted peak litter temperatures are cooler when $PAI > ln(f)/hk$).

KBDI using predicted air and litter temperatures

Using 14 sites operating over a comparable time period (December 2014–June 2015), we calculated time-averaged values of near-surface soil moisture and the four normalised KBDI metrics (K_{REF}, K_{LOC}, K_{SLA} and K_{LIT}). The results indicate a generally non-linear relationship between near-surface θ and normalised KBDI (Fig. 7), with K_{LIT} being the strongest predictor ($r^2 = 0.91$) and K_{REF} being the weakest ($r^2 = 0.63$).

KBDI results using T_{SLA} are somewhat lower than when using T_{LOC}, consistent with the effect of canopy shading, which acts to reduce daily maximum temperature and thus drying rates. A greater range of KBDI values was found when using T_{LIT} compared with T_{SLA}, consistent with the observed ranges for these two temperatures (Fig. 3).

Calculated K_{LOC}, K_{SLA} and K_{LIT} time series for north and south facing sites at two locations (Christmas Hills and Reefton) are shown in Fig. 8, exhibiting the expected pattern of rapid drying during summer (December–February) and low deficit conditions in winter (June–August). The larger north–south difference in predictions at Reefton is due to greater north–south differences in *PAI* and $\bar{S}$, compared with Christmas Hills (see Table 2).

As the KBDI is a cumulative index with a drying rate affected by temperature, any hillslope-scale variation in temperature may become amplified during dry periods, resulting in substantial site-to-site differences in estimated soil moisture deficit by the

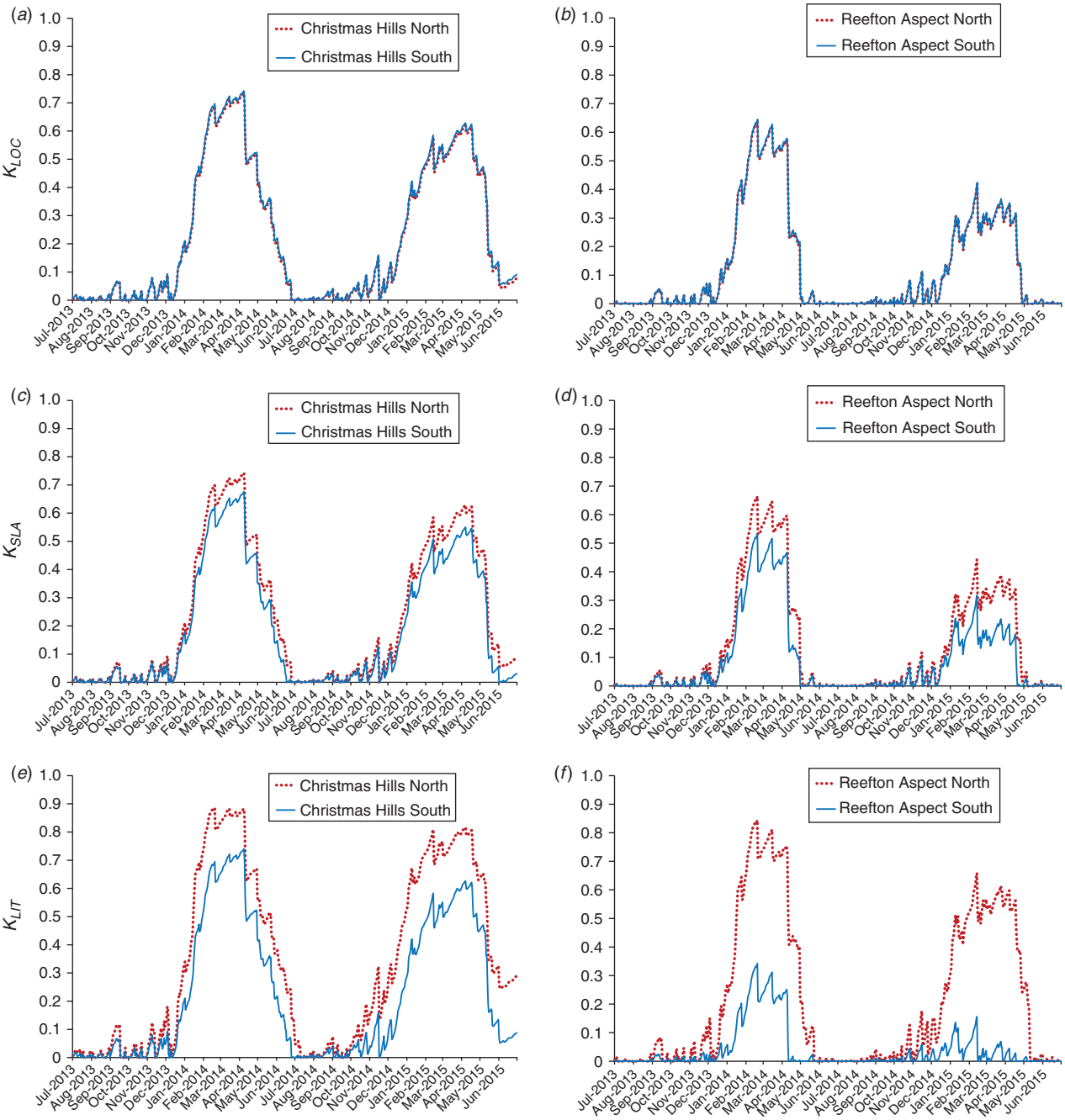

Fig. 8. Time series of normalised Keetch–Byram Drought Index (KBDI) for a 2-year period, comparing north and south facing sites at two locations – Christmas Hills (left panels), and Reefton (right panels), and comparing three metrics based on different temperature treatments: (*a*–*b*) K_{LOC}, using location-adjusted temperature; (*c*–*d*) K_{SLA}, using predicted screen-level air temperature, and (*e*–*f*) K_{LIT}, using predicted litter temperature.

end of a typical dry season. The proposed metrics K_{SLA} and K_{LIT} demonstrate such local differences, but a comparison of Fig. 8 (right panel) with Fig. 2*g* for February–April 2014 shows that K_{SLA} has somewhat underpredicted the difference between the north and south sites at Reefton, and K_{LIT} has overpredicted the effect. In contrast, at Christmas Hills, the K_{LIT} metric provides a more realistic prediction of north–south differences in moisture for February–April 2015 (Fig. 2*a*) compared with K_{SLA}.

Discussion

Temperature

At hillslope scales, topography and canopy shading interact in complex ways to affect the amount of solar radiation reaching the forest floor (Zou *et al.* 2007). In the present study, we compared several simple models of forest air and litter temperature that consider the effects of location, topographic

variation in solar radiation and canopy shading on temperature. By using physical reasoning to develop a new semi-empirical model, lower overall bias and lower aspect-specific bias were obtained in comparison with alternative simple microclimate models. The low-parameter model proposed here necessarily ignores some influences on microclimate, such as forest structure (Frey *et al.* 2016), but has the practical advantage of representing a large fraction of observed spatial variation while requiring minimal input data.

The effects of location on daily maximum temperature were assessed using site elevation and a lapse rate, with a minor adjustment for latitude. The 10-year mean lapse rate was accurately determined for the study area, but variability due to season (Stone and Carlson 1979), cloud cover (Running *et al.* 1987), hillslope position (Rolland 2003) and elevation (Grab 2013) were not assessed. In practice, the importance of these issues depends on the distance between reference and target locations. In our study area, the network of BoM temperature measurements is quite sparse, with large distances between experimental sites and reference sites (up to 42 km), thus imposing a somewhat stringent test of model performance. In forecasting applications, gridded temperature predictions would be typically available at a resolution of 5 km or less, providing a more local reference temperature and consequently reducing uncertainty in this component of the model.

In this work, the motivation for predicting forest air and litter temperatures was to examine the effects of terrain and canopy on drying rates for near-surface soil, but there may be other applications, including litter decomposition rates (Moore *et al.* 1999) and seedling establishment (von Arx *et al.* 2013). Application of the model is limited by availability of canopy density data (*PAI*), but remote sensing methods can generate very high resolution maps of vegetation (Gao *et al.* 2012; Johansen *et al.* 2012), which could be calibrated where sufficient ground-based canopy measurements exist. Although the experiments reported here have spanned a range of forest types, climates, topographic aspects and canopy densities, the parameterised models presented in Tables 4 and 5 are only valid for the study area (Fig. 1) and should not be used beyond the experimental ranges of $\bar{S}$ (0.74–1.29) and *PAI* (0.35–5.31), or in forest types that are substantially different from those at our experimental sites (Table 2).

Near-surface soil moisture deficit

Forest fire behaviour is influenced by moisture in all major fuel strata, including litter, live vegetation, bark and suspended fuels (Gould *et al.* 2011). A drought index designed to indicate the general level of forest dryness may be a poor indicator of litter moisture and the live moisture in low (near-surface) vegetation, which are the critical fuels involved in low-intensity prescribed burns. At daily time scales, near-surface soil moisture may provide a better indication of the moisture status of litter and live surface fuels (and consequently the behaviour of low-intensity fires). The results in Fig. 2 indicate strong hillslope-scale variation in near-surface soil moisture, but information on these spatial patterns is not typically available to fire risk managers.

By modifying an established drought index (KBDI), we have highlighted the potential for capturing the spatial variation in near-surface soil moisture deficit in forested environments using only simple models with a low number of parameters (Fig. 7). The KBDI was specifically developed for forests (Keetch and Byram 1968), and as such, it operates within a more constrained parameter space compared with the larger problem of a landscape with multiple vegetation types, which requires a more general approach to soil moisture (e.g. Zhang *et al.* 2001; Rodríguez-Iturbe *et al.* 2006). In addition, the modifications proposed here have focused on an easily measurable quantity, namely temperature, which simplifies the task of experimentally determining model parameters for a given region.

Nevertheless, this simple method neglects other key factors that could be expected to affect rates of near-surface soil moisture loss, including soil properties (Taufik *et al.* 2015), vapour pressure deficit (Gharun *et al.* 2014; Williams *et al.* 2015), wind speed (Jones 1992; Fisher *et al.* 2005), subsurface water movement (Lin *et al.* 2005; Lee *et al.* 2007) and drought-induced tree mortality (Hember *et al.* 2016). The extent of shallow-rooted near-surface vegetation may play a key role in determining transpiration losses from near-surface soil (Blanken *et al.* 1997), and direct evaporation may be a critical factor in some forest types, particularly where the canopy is more open (Raz-Yaseef *et al.* 2010; Schlesinger and Jasechko 2014). A further limitation is that moisture loss is represented in the KBDI with a generic function of temperature, which could be improved by using a local calibration (Garcia-Prats *et al.* 2015), although this would need to be sufficiently general to work with varying forest types.

Hillslope-scale variation in the soil wetting process is also expected in complex terrain (Nyman *et al.* 2015*b*). Reductions in effective rainfall may occur through canopy interception or litter interception, the latter possibly representing a substantial proportion of total interception in eucalypt forests (Bulcock and Jewitt 2012; Dunkerley 2015). The KBDI interception algorithm treats all canopies identically, and may eliminate a large fraction of incoming rainfall in climates where much of the rainfall occurs as light showers. Given the operational use of the KBDI across entire continents with varying forest canopies and climates, replacing the fixed-interception method with a more comprehensive algorithm (e.g. Rutter *et al.* 1971; Gash 1979; van Dijk and Bruijnzeel 2001) would be well justified, although this has not been attempted here.

A further consideration is that during wetter periods, the KBDI has a tendency to saturate, giving near-zero deficit results (Fig. 8), although observations indicate that near-surface soil moisture exhibits a broad peak over the winter months, with no clear upper limit (Fig. 2). This may be due to soil moisture loss processes that are not represented in the KBDI (e.g. vertical or lateral drainage), or to inaccuracies in the drying rate during wet conditions. For most fire behaviour applications, this is not an issue, but some caution is required when using the proposed metrics in late autumn or early winter on south facing slopes, where near-surface soil moisture levels may be approaching field saturation.

Implications for fire management

In predicting forest fire behaviour, a range of fuel strata may need to be considered, from live fuels, which are affected by moisture in the root zone (Pellizzaro *et al.* 2007), to suspended

dead fuel, which is affected by atmospheric processes only (Anderson and Anderson 2009). Our near-surface soil moisture analysis is relevant for surface fires where litter and live near-surface vegetation are the dominant fuels. It is particularly relevant to the use of prescribed fire in complex terrain, where the fine-scale spatial pattern of forest floor moisture is generally unknown but may have a considerable effect on burn outcomes.

Observations at our field sites suggest that aspect and canopy density variation in complex terrain causes large variations in near-surface soil moisture deficit at the hillslope scale. This in turn is likely to drive variations in moisture levels in litter and near-surface fuels, creating a complex mosaic of potential fire behaviour. For severe wildfires where spot-fire development is a major process (Koo *et al.* 2010), this fine-scale mosaic may act as a control on the probability of new spot-fire ignitions in fuel beds (Viegas *et al.* 2014), although how this would affect the overall spread of a severe fire is unclear.

For low-intensity prescribed fire, burn patchiness is likely to be affected by the pattern of forest floor moisture (Penman *et al.* 2007). Given the likely influence of near-surface soil moisture on litter fuel moisture, and the key role of litter moisture in burn success (Slijepcevic *et al.* 2015), the ability to predict the fine-scale spatial pattern of soil moisture deficit may be of value in the scheduling of prescribed burns. This could potentially be achieved by using the near-surface drought metrics proposed in this study, together with standard coarse-resolution gridded weather forecasts and maps of *PAI* derived from remote sensing.

Conclusions

Using only topographic information, canopy density and temperature measured at a reference location, a predictive model was developed for daily maximum temperatures under the canopy of a range of Victorian forest types in different climates, with model r^2 values of 0.95 (air) and 0.87 (litter). The proposed model was developed using physical principles (lapse rate, topographic effects on insolation and canopy light extinction) and exhibited lower bias than comparable published models, while also representing the interaction between solar energy input and canopy shading terms in a more realistic manner.

By modifying the Keetch–Byram Drought Index to utilise modelled air and litter temperatures, simple metrics were obtained for determining the first-order effects of forest microclimate on near-surface soil moisture deficit. Across 14 sites, we were able to explain 84 and 91% of observed spatial variation in near-surface soil moisture using the proposed metrics K_{SLA} and K_{LIT} respectively. Near-surface soil moisture is likely to have a key influence on the moisture of litter and near-surface fuels, which are of fundamental importance in both wildfire and prescribed fire. This work has illustrated the extent of hillslope-scale variation in near-surface soil moisture, and highlighted the potential for routine spatial predictions of near-surface soil moisture deficit in complex terrain.

Acknowledgements

This research was funded through the Victorian Government Natural Disaster Resilience Grants Scheme (NDRGS) and the Victorian Department of Environment, Land, Water and Planning (DELWP). The authors would also like to thank DELWP for providing experimental data from the Hattah and Casterton sites.

References

Agee JK, Bahro B, Finney MA, Omi PN, Sapsis DB, Skinner CN, van Wagtendonk JW, Weatherspoon CP (2000) The use of shaded fuelbreaks in landscape fire management. *Forest Ecology and Management* **127**, 55–66. doi:10.1016/S0378-1127(99)00116-4

Akaike H (1973) Information theory and an extension of the maximum likelihood principle. In 'Second international symposium on information theory', 2–8 September 1971, Tsahkadsor, Armenia, USSR. (Eds BN Petrov, F Csaki), pp. 267–281. (Akadémiai Kiadó: Budapest, Hungary)

Alexander ME (1990) Computer calculation of the Keetch–Byram Drought Index: programmers beware! *Fire Management Notes* **51**, 23–25.

Anderson HE, Rothermel RC (1965) Influence of moisture and wind upon the characteristics of free-burning fires. *Symposium (International) on Combustion* **10**, 1009–1019. doi:10.1016/S0082-0784(65)80243-0

Anderson SAJ, Anderson WR (2009) Predicting the elevated dead fine fuel moisture content in gorse (*Ulex europaeus* L.) shrub fuels. *Canadian Journal of Forest Research* **39**, 2355–2368. doi:10.1139/X09-142

Blanchi R, Leonard JE, Leicester RH (2006) Lessons learnt from post-bushfire surveys at the urban interface in Australia. *Forest Ecology and Management* **234**, S139. doi:10.1016/J.FORECO.2006.08.184

Blanken PD, Black TA, Yang PC, Neumann HH, Nesic Z, Staebler R, den Hartog G, Novak MD, Lee X (1997) Energy balance and canopy conductance of a boreal aspen forest: partitioning overstory and understory components. *Journal of Geophysical Research, D, Atmospheres* **102**, 28915–28927. doi:10.1029/97JD00193

Boone RD, Grigal DF, Sollins P, Ahrens RJ, Armstrong DE (1999) Soil sampling, preparation, archiving and quality control. In 'Standard soil methods for long-term ecological research'. (Eds GP Robertson, DC Coleman, CS Bledsoe, P Sollins) pp. 3–28. (Oxford University Press: Oxford, UK)

Bovill W, Hawthorne S, Radic J, Baillie C, Ashton A, Noske P, Lane P, Sheridan G (2015) Effectiveness of automated fuelsticks for predicting the moisture content of dead fuels in Eucalyptus forests. In 'Proceedings of the 21st international congress on modelling and simulation', 29 November–4 December 2015, Gold Coast, Qld. (Eds T Weber, MJ McPhee, RS Anderssen) pp. 201–207. (Modelling and Simulation Society of Australia and New Zealand: Gold Coast, Qld)

Bradstock RA (2008) Effects of large fires on biodiversity in south-eastern Australia: disaster or template for diversity? *International Journal of Wildland Fire* **17**, 809–822. doi:10.1071/WF07153

Bradstock RA, Hammill KA, Collins L, Price O (2010) Effects of weather, fuel and terrain on fire severity in topographically diverse landscapes of south-eastern Australia. *Landscape Ecology* **25**, 607–619. doi:10.1007/S10980-009-9443-8

Bulcock HH, Jewitt GPW (2012) Modelling canopy and litter interception in commercial forest plantations in South Africa. *Hydrology and Earth System Sciences Discussions* **9**, 8293–8333. doi:10.5194/HESSD-9-8293-2012

Burgan RE (1987) A comparison of procedures to estimate fine dead fuel moisture for fire behaviour predictions. *South African Forestry Journal* **142**, 34–40. doi:10.1080/00382167.1987.9630281

Busch FA, Niemann JD, Coleman M (2012) Evaluation of an empirical orthogonal function-based method to downscale soil moisture patterns based on topographical attributes. *Hydrological Processes* **26**, 2696–2709. doi:10.1002/HYP.8363

Cáceres MD, Martínez-Vilalta J, Coll L, Llorens P, Casals P, Poyatos R, Pausas JG, Brotons L (2015) Coupling a water balance model with forest inventory data to predict drought stress: the role of forest structural changes vs climate changes. *Agricultural and Forest Meteorology* **213**, 77–90. doi:10.1016/J.AGRFORMET.2015.06.012

Cheal D (2010) Growth stages and tolerable fire intervals for Victoria's native vegetation data sets. Victorian Department of Environment and Primary Industries, Report No. 84. (Melbourne)

Cheney NP, Gould JS, McCaw WL, Anderson WR (2012) Predicting fire behaviour in dry eucalypt forest in southern Australia. *Forest Ecology and Management* **280**, 120–131. doi:10.1016/J.FORECO.2012.06.012

Clarke MF, Avitabile SC, Brown L, Callister KE, Haslem A, Holland GJ, Kelly LT, Kenny SA, Nimmo DG, Spence-Bailey LM, Taylor RS, Watson SJ, Bennett AF (2010) Ageing mallee eucalypt vegetation after fire: insights for successional trajectories in semi-arid mallee ecosystems. *Australian Journal of Botany* **58**, 363–372. doi:10.1071/BT10051

Daly C, Halbleib M, Smith JI, Gibson WP, Doggett MK, Taylor GH, Curtis J, Pasteris PP (2008) Physiographically sensitive mapping of climatological temperature and precipitation across the conterminous United States. *International Journal of Climatology* **28**, 2031–2064. doi:10.1002/JOC.1688

de Dios VR, Fellows AW, Nolan RH, Boer MM, Bradstock RA, Domingo F, Goulden ML (2015) A semi-mechanistic model for predicting the moisture content of fine litter. *Agricultural and Forest Meteorology* **203**, 64–73. doi:10.1016/J.AGRFORMET.2015.01.002

Dimitrakopoulos AP, Bemmerzouk AM (2003) Predicting live herbaceous moisture content from a seasonal drought index. *International Journal of Biometeorology* **47**, 73–79.

Dolling K, Chu P-S, Fujioka F (2005) A climatological study of the Keetch/Byram drought index and fire activity in the Hawaiian Islands. *Agricultural and Forest Meteorology* **133**, 17–27. doi:10.1016/J.AGRFORMET.2005.07.016

Dunkerley D (2015) Percolation through leaf litter: what happens during rainfall events of varying intensity? *Journal of Hydrology* **525**, 737–746. doi:10.1016/J.JHYDROL.2015.04.039

Ferguson SA, Peterson J, Acheson A (2001) Automated, real-time predictions of cumulative smoke impacts from prescribed forest and agricultural fires. In '4th Symposium on fire and forest meteorology', 13–15 November 2001, Reno, NV, pp. 168–175. (American Meteorological Society: Reno, NV)

Finkele K, Mills GA, Beard G, Jones DA (2006) National gridded drought factors and comparison of two soil moisture deficit formulations used in prediction of Forest Fire Danger Index in Australia. *Australian Meteorological Magazine* **55**, 183–197.

Fisher JB, DeBiase TA, Qi Y, Xu M, Goldstein AH (2005) Evapotranspiration models compared on a Sierra Nevada forest ecosystem. *Environmental Modelling & Software* **20**, 783–796. doi:10.1016/J.ENVSOFT.2004.04.009

Frey SJK, Hadley AS, Johnson SL, Schulze M, Jones JA, Betts MG (2016) Spatial models reveal the microclimatic buffering capacity of old-growth forests. *Science Advances* **2**, e1501392. doi:10.1126/SCIADV.1501392

Fujioka FM (1991) Starting up the Keetch–Byram drought index. In 'Proceedings of the 11th Conference on Fire and Forest Meteorology', 16–19 April 1991, Missoula, MT. (Eds PL Andrews, DF Potts) pp. 74–80. (Society of American Foresters: Missoula, MT)

Gao F, Anderson MC, Kustas WP, Wang Y (2012) Simple method for retrieving Leaf Area Index from Landsat using MODIS Leaf Area Index products as reference. *Journal of Applied Remote Sensing* **6**, 063554. doi:10.1117/1.JRS.6.063554

Garcia-Prats A, Antonio DC, Tarcísio FJG, Antonio MJ (2015) Development of a Keetch and Byram-based drought index sensitive to forest management in Mediterranean conditions. *Agricultural and Forest Meteorology* **205**, 40–50. doi:10.1016/J.AGRFORMET.2015.02.009

Gash JHC (1979) An analytical model of rainfall interception by forests. *Quarterly Journal of the Royal Meteorological Society* **105**, 43–55. doi:10.1002/QJ.49710544304

Geiger R, Aron RH, Todhunter P (1995) 'The climate near the ground.' (Vieweg: Braunschweig, Germany).

Gharun M, Vervoort RW, Turnbull TL, Adams MA (2014) A test of how coupling of vegetation to the atmosphere and climate spatial variation affects water yield modelling in mountainous catchments. *Journal of Hydrology* **514**, 202–213. doi:10.1016/J.JHYDROL.2014.04.037

Gill AM, Groves RH, Noble IR (1981) 'Fire and the Australian biota.' (Australian Academy of Science: Canberra, ACT).

Gould JS, McCaw WL, Cheney NP (2011) Quantifying fine fuel dynamics and structure in dry eucalypt forest (*Eucalyptus marginata*) in Western Australia for fire management. *Forest Ecology and Management* **262**, 531–546. doi:10.1016/J.FORECO.2011.04.022

Grab SW (2013) Fine-scale variations of near-surface-temperature lapse rates in the Hiah Drakensberg Escarpment, South Africa: environmental implications. *Arctic, Antarctic, and Alpine Research* **45**, 500–514. doi:10.1657/1938-4246-45.4.500

Grayson RB, Western AW, Chiew FHS (1997) Preferred states in spatial soil moisture patterns: local and non-local controls. *Water Resources Research* **33**, 2897–2908. doi:10.1029/97WR02174

Groisman PY, Sherstyukov BG, Razuvaev VN, Knight RW, Enloe JG, Stroumentova NS, Whitfield PH, Førland E, Hannsen-Bauer I, Tuomenvirta H, Aleksandersson H, Mescherskaya AV, Karl TR (2007) Potential forest fire danger over northern Eurasia: changes during the 20th century. *Global and Planetary Change* **56**, 371–386. doi:10.1016/J.GLOPLACHA.2006.07.029

Hatton TJ, Viney NR, Catchpole EA, De Mestre NJ (1988) The influence of soil moisture on eucalyptus leaf litter moisture. *Forest Science* **34**, 292–301.

Hember RA, Kurz WA, Coops NC (2016) Relationships between individual-tree mortality and water-balance variables indicate positive trends in water stress-induced tree mortality across North America. *Global Change Biology* . doi:10.1111/GCB.13428

Hwang T, Band L, Hales TC (2009) Ecosystem processes at the watershed scale: extending optimality theory from plot to catchment. *Water Resources Research* **45**, W11425. doi:10.1029/2009WR007775

Janis MJ, Johnson MB, Forthun G (2002) Near-real time mapping of Keetch–Byram drought index in the south-eastern United States. *International Journal of Wildland Fire* **11**, 281–289. doi:10.1071/WF02013

Jarvis PG, Leverenz JW (1983) Productivity of temperate, deciduous and evergreen forests. In 'Physiological plant ecology IV – ecosystem processes: mineral cycling, productivity and Man's influence'. (Eds OL Lange, PS Nobel, CB Osmond, H Ziegler) pp. 233–280. (Springer: Berlin)

Johansen K, Gill T, Trevithick R, Armston J, Scarth P, Flood N, Phinn S (2012) Landsat-based persistent green-vegetation fraction for Australia. In '16th Australasian remote sensing and photogrammetry conference', 27–29 August 2012, Melbourne, Vic. (International Society for Photogrammetry and Remote Sensing: Melbourne, Vic.)

Jones DA, Wang W, Fawcett R (2009) High-quality spatial climate datasets for Australia. *Australian Meteorological and Oceanographic Journal* **58**, 233–248.

Jones HG (1992) 'Plants and microclimate: a quantitative approach to environmental plant physiology.' (Cambridge University Press: Cambridge, UK).

Kang S, Lee D, Kimball JS (2004) The effects of spatial aggregation of complex topography on hydroecological process simulations within a rugged forest landscape: development and application of a satellite-based topoclimatic model. *Canadian Journal of Forest Research* **34**, 519–530. doi:10.1139/X03-213

Keetch JJ, Byram GM (1968) A drought index for forest fire control. USDA Forest Service, Southeastern Forest Experiment Station, Research Paper SE-38. (Asheville, NC)

Koo E, Pagni PJ, Weise DR, Woycheese JP (2010) Firebrands and spotting ignition in large-scale fires. *International Journal of Wildland Fire* **19**, 818–843. doi:10.1071/WF07119

Korres W, Reichenau TG, Fiener P, Koyama CN, Bogena HR, Cornelissen T, Baatz R, Herbst M, Diekkrüger B, Vereecken H, Schneider K (2015) Spatiotemporal soil moisture patterns – A meta-analysis using plot to

catchment scale data. *Journal of Hydrology* **520**, 326–341. doi:10.1016/J.JHYDROL.2014.11.042

Krueger ES, Ochsner TE, Carlson JD, Engle DM, Twidwell D, Fuhlendorf SD (2016) Concurrent and antecedent soil moisture relate positively or negatively to probability of large wildfires depending on season. *International Journal of Wildland Fire* **25**, 657–668. doi:10.1071/WF15104

Kutiel P, Lavee H (1999) Effect of slope aspect on soil and vegetation properties along an aridity transect. *Israel Journal of Plant Sciences* **47**, 169–178. doi:10.1080/07929978.1999.10676770

Lee H, Zehe E, Sivapalan M (2007) Predictions of rainfall-runoff response and soil moisture dynamics in a microscale catchment using the CREW model. *Hydrology and Earth System Sciences* **11**, 819–849. doi:10.5194/HESS-11-819-2007

Lee R (1978) 'Forest microclimatology.' (Columbia University Press: New York).

Lin H, Bouma J, Wilding LP, Richardson JL, Kutílek M, Nielsen DR (2005) Advances in hydropedology. In 'Advances in agronomy'. (Ed. DL Sparks) Vol. 85, pp. 1–89. (Elsevier Academic Press: San Diego, CA)

Liu Y, Stanturf J, Goodrick S (2010) Trends in global wildfire potential in a changing climate. *Forest Ecology and Management* **259**, 685–697. doi:10.1016/J.FORECO.2009.09.002

Lucas C (2010) On developing a historical fire weather data-set for Australia. *Australian Meteorological and Oceanographic Journal* **60**, 1–14.

Martell DL, Sun H (2008) The impact of fire suppression, vegetation, and weather on the area burned by lightning-caused forest fires in Ontario. *Canadian Journal of Forest Research* **38**, 1547–1563. doi:10.1139/X07-210

Matthews S (2014) Dead fuel moisture research: 1991–2012. *International Journal of Wildland Fire* **23**, 78–92. doi:10.1071/WF13005

McArthur AG (1967) Fire behaviour in eucalypt forests. Forestry and Timber Bureau, Leaflet No. 107. (Canberra, ACT)

Moore ID, Norton TW, Williams JE (1993) Modelling environmental heterogeneity in forested landscapes. *Journal of Hydrology* **150**, 717–747. doi:10.1016/0022-1694(93)90133-T

Moore TR, Trofymow JA, Taylor B, Prescott C, Camiré C, Duschene L, Fyles J, Kozak L, Kranabetter M, Morrison I, Siltanen M, Smith S, Titus B, Visser S, Wein R, Zoltai S (1999) Litter decomposition rates in Canadian forests. *Global Change Biology* **5**, 75–82. doi:10.1046/J.1365-2486.1998.00224.X

Nelson RM (1959) Drought estimation in southern forest fire control. USDA Forest Service, Southeastern Forest Experiment Station, Paper 99. (Asheville, NC)

Nesterov VG (1949) 'Combustibility of the forest and methods for its determination.' (USSR State Industry Press: Moscow).

Noble IR, Slatyer RO (1981) Concepts and models of succession in vascular plant communities subject to recurrent fire. In 'Fire and the Australian biota'. (Eds AM Gill, RH Groves, IR Noble) (Australian Academy of Science: Canberra, ACT)

Noble IR, Bary GAV, Gill AM (1980) McArthur's fire-danger meters expressed as equations. *Australian Journal of Ecology* **5**, 201–203. doi:10.1111/J.1442-9993.1980.TB01243.X

Nyman P, Sherwin CB, Langhans C, Lane PNJ, Sheridan GJ (2014) Downscaling regional climate data to calculate the radiative index of dryness in complex terrain. *Australian Meteorological and Oceanographic Journal* **64**, 109–122.

Nyman P, Baillie C, Bovill W, Lane P, Tolhurst K, Duff T, Sheridan G (2015*a*) Measurement of topographic controls on the moisture content of surface fuels in south-east Australian forests. In 'Proceedings of the 21st international congress on modelling and simulation', 29 November–4 December 2015, Gold Coast, Qld. (Eds T Weber, MJ McPhee, RS Anderssen) pp. 264–269. (Modelling and Simulation Society of Australia and New Zealand: Gold Coast, Queensland)

Nyman P, Metzen D, Noske PJ, Lane PNJ, Sheridan GJ (2015*b*) Quantifying the effects of topographic aspect on water content and temperature in fine surface fuel. *International Journal of Wildland Fire* **24**, 1129–1142. doi:10.1071/WF14195

Pellizzaro G, Cesaraccio C, Duce P, Ventura A, Zara P (2007) Relationships between seasonal patterns of live fuel moisture and meteorological drought indices for Mediterranean shrubland species. *International Journal of Wildland Fire* **16**, 232–241. doi:10.1071/WF06081

Penman TD, Kavanagh RP, Binns DL, Melick DR (2007) Patchiness of prescribed burns in dry sclerophyll eucalypt forests in south-eastern Australia. *Forest Ecology and Management* **252**, 24–32. doi:10.1016/J.FORECO.2007.06.004

R Development Core Team (2014) 'A language and environment for statistical computing.' (R Foundation for Statistical Computing: Vienna, Austria)

Raz-Yaseef N, Rotenberg E, Yakir D (2010) Effects of spatial variations in soil evaporation caused by tree shading on water flux partitioning in a semi-arid pine forest. *Agricultural and Forest Meteorology* **150**, 454–462. doi:10.1016/J.AGRFORMET.2010.01.010

Reid AM, Robertson KM, Hmielowski TL (2012) Predicting litter and live herb fuel consumption during prescribed fires in native and old-field upland pine communities of the south-eastern United States. *Canadian Journal of Forest Research* **42**, 1611–1622. doi:10.1139/X2012-096

Rich P, Wood J, Vieglais D, Burek K, Webb N (1999) 'Guide to HemiView: software for analysis of hemispherical photography.' (Delta-T Devices, Ltd: Cambridge, UK)

Riley KL, Abatzoglou JT, Grenfell IC, Klene AE, Heinsch FA (2013) The relationship of large fire occurrence with drought and fire danger indices in the western USA, 1984–2008: the role of temporal scale. *International Journal of Wildland Fire* **22**, 894–909. doi:10.1071/WF12149

Rodríguez-Iturbe I, Isham V, Cox DR, Manfreda S, Porporato A (2006) Space–time modeling of soil moisture: stochastic rainfall forcing with heterogeneous vegetation. *Water Resources Research* **42**, W06D05. doi:10.1029/2005WR004497

Rolland C (2003) Spatial and seasonal variations of air temperature lapse rates in Alpine regions. *Journal of Climate* **16**, 1032–1046. doi:10.1175/1520-0442(2003)016<1032:SASVOA>2.0.CO;2

Running SW (1991) Computer simulation of regional evapotranspiration by integrating landscape biophysical attributes with satellite data. In 'Land surface evaporation'. (Eds TJ Schmugge, J-C André) pp. 359–369. (Springer: New York)

Running SW, Nemani RR, Hungerford RD (1987) Extrapolation of synoptic meteorological data in mountainous terrain and its use for simulating forest evapotranspiration and photosynthesis. *Canadian Journal of Forest Research* **17**, 472–483. doi:10.1139/X87-081

Rutter AJ, Kershaw KA, Robins PC, Morton AJ (1971) A predictive model of rainfall interception in forests, 1. Derivation of the model from observations in a plantation of Corsican pine. *Agricultural Meteorology* **9**, 367–384. doi:10.1016/0002-1571(71)90034-3

Schlesinger WH, Jasechko S (2014) Transpiration in the global water cycle. *Agricultural and Forest Meteorology* **189–190**, 115–117. doi:10.1016/J.AGRFORMET.2014.01.011

Schunk C, Wastl C, Leuchner M, Schuster C, Menzel A (2013) Forest fire danger rating in complex topography – results from a case study in the Bavarian Alps in autumn 2011. *Natural Hazards and Earth System Sciences* **13**, 2157–2167. doi:10.5194/NHESS-13-2157-2013

Sharma C, Gairola S, Baduni N, Ghildiyal S, Suyal S (2011) Variation in carbon stocks on different slope aspects in seven major forest types of temperate region of Garhwal Himalaya, India. *Journal of Biosciences* **36**, 701–708. doi:10.1007/S12038-011-9103-4

Sharples JJ (2009) An overview of mountain meteorological effects relevant to fire behaviour and bushfire risk. *International Journal of Wildland Fire* **18**, 737–754. doi:10.1071/WF08041

Slijepcevic A, Anderson WR, Matthews S (2013) Testing existing models for predicting hourly variation in fine fuel moisture in eucalypt forests. *Forest Ecology and Management* **306**, 202–215. doi:10.1016/J.FORECO.2013.06.033

Slijepcevic A, Anderson WR, Matthews S, Anderson DH (2015) Evaluating models to predict daily fine fuel moisture content in eucalypt forest. *Forest Ecology and Management* **335**, 261–269. doi:10.1016/J.FORECO.2014.09.040

Stone PH, Carlson JH (1979) Atmospheric lapse rate regimes and their parameterization. *Journal of the Atmospheric Sciences* **36**, 415–423. doi:10.1175/1520-0469(1979)036<0415:ALRRAT>2.0.CO;2

Sullivan AL, McCaw WL, Cruz MG, Matthews S, Ellis PF (2012) Fuel, fire weather and fire behaviour in Australian ecosystems. In 'Flammable Australia: fire regimes, biodiversity and ecosystems in a changing world'. (Eds RA Bradstock, AM Gill, RJ Williams) pp. 51–77. (CSIRO Publishing: Melbourne)

Svetlitchnyi AA, Plotnitskiy SV, Stepovaya OY (2003) Spatial distribution of soil moisture content within catchments and its modelling on the basis of topographic data. *Journal of Hydrology* **277**, 50–60. doi:10.1016/S0022-1694(03)00083-0

Taufik M, Setiawan BI, van Lanen HAJ (2015) Modification of a fire drought index for tropical wetland ecosystems by including water table depth. *Agricultural and Forest Meteorology* **203**, 1–10. doi:10.1016/J.AGRFORMET.2014.12.006

Torok SJ, Morris CJ, Skinner C, Plummer N (2001) Urban heat island features of south-east Australian towns. *Australian Meteorological Magazine* **50**, 1–13.

van Dijk AIJM, Bruijnzeel LA (2001) Modelling rainfall interception by vegetation of variable density using an adapted analytical model. Part 1. Model description. *Journal of Hydrology* **247**, 230–238. doi:10.1016/S0022-1694(01)00392-4

van Dijk AIJM, Renzullo LJ (2011) Water resource monitoring systems and the role of satellite observations. *Hydrology and Earth System Sciences* **15**, 39–55. doi:10.5194/HESS-15-39-2011

Van Wagner CE (1987) Development and structure of the Canadian Forest Fire Weather Index System. Canadian Forestry Service, Technical Report No. 35. (Ottawa, ON)

Varol T, Ertuğrul M (2016) Analysis of the forest fires in the Antalya region of Turkey using the Keetch–Byram drought index. *Journal of Forest Research* **27**, 811–819. doi:10.1007/S11676-016-0235-0

Viegas D, Almeida M, Raposo J, Oliveira R, Viegas C (2014) Ignition of Mediterranean fuel beds by several types of firebrands. *Fire Technology* **50**, 61–77. doi:10.1007/S10694-012-0267-8

Viney NR (1991) A review of fine-fuel moisture modelling. *International Journal of Wildland Fire* **1**, 215–234. doi:10.1071/WF9910215

von Arx G, Graf Pannatier E, Thimonier A, Rebetez M (2013) Microclimate in forests with varying Leaf Area Index and soil moisture: potential implications for seedling establishment in a changing climate. *Journal of Ecology* **101**, 1201–1213. doi:10.1111/1365-2745.12121

Western AW, Grayson RB, Bloschl G (2002) Scaling of soil moisture: a hydrologic perspective. *Annual Review of Earth and Planetary Sciences* **30**, 149–180. doi:10.1146/ANNUREV.EARTH.30.091201.140434

Williams AP, Seager R, Macalady AK, Berkelhammer M, Crimmins MA, Swetnam TW, Trugman AT, Buenning N, Noone D, McDowell NG, Hryniw N, Mora CI, Rahn T (2015) Correlations between components of the water balance and burned area reveal new insights for predicting forest fire area in the south-west United States. *International Journal of Wildland Fire* **24**, 14–26. doi:10.1071/WF14023

Wilson JP, Gallant JC (2000) Secondary topographic attributes. In 'Terrain analysis: principles and applications'. (Eds JP Wilson, JC Gallant) pp. 87–131. (Wiley: New York)

Xanthopoulos G, Maheras G, Gouma V, Gouvas M (2006) Is the Keetch–Byram drought index (KBDI) directly related to plant water stress? 'Proceedings of the V international conference on forest fire research', 27–30 November 2006, Coimbra, Portugal. (Ed. DX Viegas) (ADAI (Associaçao para o Desenvolvimento da Aerodinamica Industrial): Coimbra, Portugal)

Zhang L, Dawes WR, Walker GR (2001) Response of mean annual evapotranspiration to vegetation changes at catchment scale. *Water Resources Research* **37**, 701–708. doi:10.1029/2000WR900325

Zou CB, Barron-Gafford GA, Breshears DD (2007) Effects of topography and woody plant canopy cover on near-ground solar radiation: relevant energy inputs for ecohydrology and hydropedology. *Geophysical Research Letters* **34**, L24S21. doi:10.1029/2007GL031484